Spectral tuning in the eyes of deep-sea lanternfishes (Myctophidae): a novel sexually dimorphic intra-ocular filter

Fanny de Busserolles[1,2,3], Nathan S. Hart[1], David M. Hunt[1,4], Wayne I. Davies[1], N. Justin Marshall[2], Michael W. Clarke[5], Dorothee Hahne[5], Shaun P. Collin[1,4].

1. School of Animal Biology and the Oceans Institute, The University of Western Australia, Perth, Crawley WA 6009, Australia.
2. Sensory Neurobiology Group, Queensland Brain Institute, University of Queensland, Brisbane, QLD, Australia.
3. Red Sea Research Centre, King Abdullah University of Science and Technology, Thuwal 23955-6900, Saudi Arabia.
4. Lions Eye Institute, The University of Western Australia, Perth, WA, Australia
5. UWA Centre for Metabolomics, Metabolomics Australia, The University of Western Australia, Perth, WA, Australia.

Running head title: Spectral tuning in lanternfishes

Number of figures: 8

Number of tables: 2

Full address of corresponding author:

Queensland Brain Institute

University of Queensland

St. Lucia, Brisbane, QLD 4072, Australia

fanny.debusserolles@kaust.edu.sa

Key words: yellow pigment, retinal filter, spectral tuning, myctophids, deep-sea, opsins, microspectrophotometry, bioluminescence, sexual dimorphism.

Abstract

Deep-sea fishes possess several adaptations to facilitate vision, where light detection is pushed to its limit. Lanternfishes (Myctophidae), one of the world's most abundant groups of mesopelagic fishes, possess a novel and unique visual specialisation, a sexually dimorphic photostable yellow pigmentation, constituting the first record of a visual sexual dimorphism in any non-primate vertebrate. The topographic distribution of the yellow pigmentation across the retina is species-specific, varying in location, shape and size. Spectrophotometric analyses reveal this new retinal specialisation differs between species in terms of composition and acts as a filter, absorbing maximally between 356 nm and 443 nm. Microspectrophotometry and molecular analyses indicate that the species containing this pigmentation also possess at least two spectrally distinct rod visual pigments, as a result of a duplication of the *Rh1* opsin gene. After modelling the effect of the yellow pigmentation on photoreceptor spectral sensitivity, we suggest that this unique specialisation acts as a filter to enhance contrast, thereby improving the detection of bioluminescent emissions and possibly fluorescence in the extreme environment of the deep-sea. The fact that this yellow pigmentation is species-specific, sexually dimorphic and isolated within specific parts of the retina indicates an

evolutionary pressure to visualise prey/predators/mates in a particular part of each species' visual field.

Introduction

The evolution of visual sensitivity appears to be driven primarily by the spectral range and intensity of available light within a species' visual environment. As a result, different visual pigments are found in the retina of different species, with spectral sensitivities broadly matching the surrounding light conditions [Lythgoe and Partridge, 1989]. Spectral adaptation to the photic environment is mainly achieved by two types of tuning mechanisms: variation in the number of spectral classes of photoreceptors through the loss or duplication of opsin genes, and variation in the type of chromophore within the photoreceptor outer segment (see [Bowmaker and Hunt, 2006; Bowmaker, 2008; Davies et al., 2012] for review).

Due to the physical properties of water, aquatic animals can be found in a wide range of spectral environments, from clear blue oceanic water to turbid brown river water, and, as a result, possess different subsets of cone classes, ranging from the presence of at least one representative of each of the four cone classes (Australian lungfish, [Bailes et al., 2007]) at one extreme, to the retention of just a single cone class (several species of sharks, [Hart et al., 2011]) at the other, although it is not uncommon amongst deep-sea fishes to find that all four cone classes have been lost to leave a rod-only retina [Hunt et al., 2001]. In the open ocean, light conditions vary greatly with depth, decreasing in intensity and spectral range as the short and long wavelengths are attenuated. In the deep-sea, only very low intensities of sunlight in the blue-green range

remain below 200 m, creating a relatively dark environment accompanied by a multitude of bioluminescent emissions that are also mainly concentrated in the blue-green part of the visible light spectrum [Widder, 2002; 2010].

The eyes of deep-sea teleost fishes represent a good example of visual adaptation in spectral sensitivity. Most species have adapted to their dim-light environment by losing their cone photoreceptors (photic vision) in favour of a single type of rod photoreceptor (scotopic vision) containing a single visual pigment, encoded by the *Rh1* rod opsin gene. While most terrestrial and shallow water vertebrates usually have an *Rh1* visual pigment maximally absorbing around 500 nm, many deep-sea teleosts have shifted the spectral sensitivity of their rod pigment towards shorter wavelengths to spectrally match their ambient photic environment, i.e. maximal absorbance around 480 nm [Crescitelli, 1990; Douglas and Partridge, 1997; Douglas et al., 2003]. The tuning mechanism responsible for the spectral shift toward shorter wavelengths in the *Rh1* gene has been identified at the molecular level and occurs as a result of different combinations of substitutions at eight different amino acid sites depending on the species [Hunt et al., 2001].

Like most mesopelagic fishes, lanternfishes (Myctophidae) possess several visual adaptations for life in the mesopelagic zone that serve to increase the sensitivity of the eye and optimise photon capture [de Busserolles et al., 2013; de Busserolles et al., 2014a; de Busserolles et al., 2014b]. Lanternfishes generally lack cones and possess a single rod photoreceptor class with a peak spectral absorption tuned to the blue-green region of the visible spectrum [Partridge et al., 1992; Douglas and Partridge, 1997; Turner et al., 2009]. However, the presence of two photoreceptor classes has been found in a few

93 species [Hasegawa et al., 2008; Turner et al., 2009]. In this study, we describe a novel
94 visual adaptation, a retinal yellow pigmentation associated with a rod gene duplication,
95 that is unique among vertebrates and assists lanternfishes to tune their visual sensitivity.
96
97 **Material and methods**
98 ***Samples***
99 Samples were collected in the Coral Sea during three cruises on the RV *Cape*
100 *Ferguson* (AIMS, Townsville, Australia) in Autumn-Winter 2010-2012 under the
101 following collection permits: Coral Sea waters (CSCZ-SR-20091001-01),
102 Commonwealth waters (AU-COM2009051), GBRMPA (G09/32237.1) and Queensland
103 Fisheries (133805), (Marshall, AEC # SNG/080/09/ARC). Sampling was performed at
104 the surface (<5 m) during the night using an Isaacs-Kid Midwater Trawl fitted with
105 buoys. For each individual, the standard length and rostro-caudal eye diameter were
106 measured with digital callipers (to a precision of 0.1 mm) prior to dissection and fixation
107 (Table 1). Following the guidelines of the NH&MRC Australian Code of Practice, under
108 our University of Western Australia Animal Ethic protocol (RA/3/100/917), eyes were
109 then enucleated, the cornea and lens were dissected free from the eye cup and tissue fixed
110 specifically for different analyses (4% paraformaldehyde, RNALater, 100% alcohol,
111 liquid nitrogen). One individual of *Myctophum brachygnathum*, sampled in Hawaii in
112 May 2011 and fixed in 5% formalin, was provided by the American Museum of Natural
113 History, New York, USA (Table 1).
114
115 ***Retinal wholemounts and spectrophotometry***

For each species, eyes preserved in 4% paraformaldehyde in 0.1M sodium phosphate buffer (pH 7.4, PFA) were dissected to reveal the location and shape of the yellow pigmented patches of retinal tissue. Retinal wholemounts were made according to standard protocols [Stone, 1981; Coimbra et al., 2006, Ullmann et al. 2011] and mounted photoreceptor side up in 0.1M phosphate buffer (pH 7.4) between two No. 1 glass coverslips. For one specimen of *Symbolophorus rufinus*, the eye was dissected on board ship directly after capture and the retina wholemounted fresh in between two No. 1 coverslips and kept at -20°C in a light-tight container until analysis.

The transmission of light (300-800 nm) through each retina was measured systematically every 0.5 mm or 1 mm (depending of the size of the retina) across the wholemount using spectrophotometry. Each transmission spectrum was ultimately converted to a corrected absorbance spectra at the wavelength of maximum absorbance of the yellow pigment (λ_{YPmax}). The detailed methods used to carry out the spectrophotometry analyses are provided in the Supplementary Material. The λ_{YPmax} values were then mapped on to an outline of the retinal wholemount traced from the calibrated digital image in Adobe Illustrator CS4. The whole file was saved as a scalable vector graphics (.svg) file and imported into R v.2.15.0 (R Foundation for Statistical Computing 2012) to construct the maps using custom scripts [Garza Gisholt et al., 2014]. For this study, the Gaussian Kernel Smoother from the Spatstat package was used to construct the iso-density maps [Baddeley and Turner, 2005]. For each map, the sigma value was adjusted to 30.

Cryosections

The retina of one individual of *Gonichthys tenuiculus*, preserved in 4% PFA, was processed for cryosectioning in order to visualise the position of the yellow pigmentation within the retina. Sections (40 µm in thickness) were cut using a Leica CM1900 cryostat-microtome and mounted in VectaMount Aqueous medium (Vector Laboratories, CA, USA). The sections were observed under an Olympus BX50 compound light microscope and pictures taken with an Olympus DP70 digital camera.

Identification of the yellow pigmentation

Yellow pigments have previously been observed in the eyes of vertebrates, either as a diffuse pigment within the lens and cornea or within the inner segment of the photoreceptors i.e. in oil droplets or ellipsoids [Muntz, 1976; Appleby and Muntz, 1979; Goldsmith et al., 1984; Collin et al., 2003; Siebeck et al. 2003; Bailes et al. 2006]. These pigments have been identified as tryptophan derivatives [van Heyningen, 1971a, b; Thorpe et al., 1992] or mycosporine-like amino acids [Thorpe et al., 1993] in the lens, and as carotenoids [Goldsmith et al., 1984] in the retina. Extraction methods for the yellow pigment found in the retina of the lanternfishes followed therefore the classic extraction protocols for these various group of compounds, using appropriate standards. Retinae of *Myctophum aurolaternatun* and *Hygophum proximum* were dissected while onboard ship, deep-frozen in liquid nitrogen in small eppendorf tubes and stored at -20°C. In order to extract any water-soluble pigments (e.g. tryptophan derivatives and other amino acids), the retina of *M. aurolaternatum* was thawed at room temperature and homogenised several times in a glass tube with 1 ml of distilled water (3 mins at 30Hz) [Truscott et al. 1992; Thorpe et al. 1993]. Extraction of possible carotenoids was

performed as described by Toomey and McGraw [2007, 2009]. The retina of *H. proximum* was thawed and 10 µl of Trans-β-Apo-8-Carotenal (1ng/µl, Sigma Aldrich) and 50µl of retinyl acetate (1ng/µl, Sigma Aldrich) were added to the sample as internal standards. The sample was then homogenised in 1ml of methanol for 3 mins at 30Hz, centrifuged (3mins at 13000 rpm) and the supernatant transferred into a glass tube. The procedure was repeated twice with 1 ml of 1:1 hexane:*tert*-butyl methyl ether (MTBE) and the supernatants combined. Since the yellow pigment was still present in the tissue and not in the supernatant, we repeated the procedure twice more with 1 ml of dimethyl sulfoxide (DMSO) [Sedmak et al. 1990].

Microspectrophotometry

The eyes of three species of lanternfishes, *Myctophum obtusirostre*, *M. spinosum* and *Symbolophorus evermanni*, were preserved for microspectrophotometry (MSP) according to Hart et al. [2011]. Specimens were collected alive and were dark adapted for 15 mins before being euthanized following the guidelines of the NH&MRC Australian Code of Practice, under the University of Western Australia Animal Ethics protocol (RA/3/100/917). Eyes were removed in the dark under dim red light, the cornea removed and the whole eye lightly fixed for 30 seconds in 2.5% glutaraldehyde in phosphate buffered saline (PBS, 340 mOsmol kg^{-1}, pH 7.0), washed in PBS for 30 s and stored in PBS at 4°C in a light-tight container until they were analysed back in the laboratory, three to four weeks later.

In all cases, small pieces (ca. 1x1 mm to 3x3 mm) of retina were mounted between No. 1 glass coverslips in a drop of 425 mOsmol kg^{-1} PBS containing 10%

dextran (MW 282,000; Sigma D-7265). Absorbance spectra (330–800 nm) were made using a computer-controlled single-beam wavelength-scanning microspectrophotometer [Hart et al., 2004; 2011; 2012]. Due to the very small diameter of the rod photoreceptors of the lanternfish species analysed (<1 μm [de Busserolles et al., 2014b]), longitudinal "end-on" absorbance spectra were measured from patches of rod outer segments. A sample scan was made by aligning the measuring beam (typical dimensions 10 ×10 μm) within a patch of rods in a specific part of the retina and recording the amount of light transmitted at each wavelength across the spectrum. Baseline scans were made in an identical way to sample scans but from a cell-free area of the preparation. The transmittance (ratio of sample to baseline signal) of the outer segments was calculated at each wavelength and converted to absorbance to give a prebleach spectrum. Each patch of rods was then bleached with broadband white light for 2 min and subsequent sample and baseline scans were made to create a postbleach absorbance spectrum. Because we were measuring the absorbance through a patch of retina that contains other absorbing material (i.e. other retinal layers, yellow pigment) and not through a single rod outer segment, a difference spectrum was calculated by subtracting the postbleach scan from the prebleach scan. Only spectra that satisfied established selection criteria [Levine and MacNichol Jr, 1985; Hart et al., 1998] were retained for further analysis. Difference absorbance spectra were analysed as described elsewhere [MacNichol Jr, 1986; Govardovskii et al., 2000; Hart, 2002] to provide an estimate of the wavelength of maximum absorbance (λ_{max}) of the retinal pigment contained in the rods, assuming that only one type of rod was present within the patch analysed. The mean λ_{max} of a given pigment was then calculated from these individual patch λ_{max} values. For display

purposes, a mean difference absorbance spectrum was calculated by averaging the acceptable individual absorbance spectra.

To investigate the possibility that the photoreceptors of some species contained a mixture of visual pigment molecules utilising both the A_1 and A_2 chromophores, mean prebleach absorbance spectra (smoothed with a variable point unweighted running average) were fitted iteratively using the Excel Solver function in a custom macro written by NSH with mixed-chromophore pigment templates to find the combination of visual pigment λ_{max} (pure A_1) and A_1/A_2 ratio that gave the smallest sums of squares deviation between the real and modelled spectra between 0.8 and 0.2 normalised absorbance on the long-wavelength limb of the real spectrum (approximately the same region used to estimate λ_{max}; [Temple et al., 2010]. We made the assumption that only a single type of visual pigment opsin protein was expressed in each rod within the patch of rods and used established A_1 and A_2 visual pigment templates [Govardovskii et al., 2000] and a known relationship between the λ_{max} values of A_1 and A_2 visual pigment pairs [Parry and Bowmaker, 2000].

Molecular analyses

Eye and muscle tissue from *S. evermanni* were preserved for molecular analyses by immersion in RNALater and 100% alcohol, respectively, followed by storage at -20^{o}C. Genomic DNA (gDNA) was extracted from the muscle tissue using the DNeasy Blood & Tissue Kit (Qiagen), following the protocol provided by the manufacturer. First-round PCR amplifications utilised the "All-Opsins, All-Species" (AOAS) degenerate PCR primer set F1/R2 designed by Davies et al. [2009]. A second hemi-nested PCR was

carried out with primer sets F1/R1 and F2/R2 [Davies et al., 2009]. The sequences of the primers used in this study along with the annealing temperatures used and expected PCR products are provided in the Supplementary Material (Table S1).

RNA was extracted from eye tissue using the PureLink RNA Mini Kit (Invitrogen) and cDNA synthesised using the 5'/3' RACE Kit 2nd generation (Roche) according to the manufacturer's instructions. Opsin sequences were amplified from cDNA using primer sets designed to amplify vertebrate opsins. The resulting amplified fragments were sequenced and the sequences used to design primers for RACE in order to extend the sequences at the 3' ends.

All PCR amplifications were performed using a HotStarTaq DNA Polymerase Kit (Qiagen). Following a heat-activation step of 15 mins at 95°C, 45 cycles were performed with a denaturation step of 30 s at 94°C, an annealing step of 60 s at 45-50°C, an extension step of 90 s at 72°C and a final extension of 10 mins at 72°. Gel-purified (Wizard SV Gel and PCR Clean-up System, Promega) PCR products were sequenced by the Sanger method.

Phylogenetic trees, including the *S. evermanni* opsin genes sequenced in this study, were constructed by Neighbour-Joining [Saitou and Nei, 1987] and Maximum Likelihood using nucleotide sequences. All sequences were aligned in Clustal Omega [Sievers et al., 2011] and refined by eye. The parameters for the phylogenetic analysis, carried out using the MEGA phylogenetic package [Tamura et al., 2013], were pair-wise deletion and Kimura 2-parameter correction. The degree of support for internal branching was assessed by bootstrapping with 1000 replicates.

Modelling of the association of the yellow pigment and the visual pigments

The effect of the yellow pigmentation on the spectral sensitivity of the rods was modelled for two species, *M. obtusirostre* and *S. evermanni*. For each species, the quantal spectral sensitivity of the rod photoreceptors associated with the yellow pigmentation was modelled by multiplying the species-specific axial spectral absorptance of the rod outer segment by the spectral transmittance of the species-specific overlying yellow pigmentation. We used visual pigment templates [Govardovskii et al., 2000] of appropriate λ_{max} for the modelling. Normalized absorbance templates were converted to axial outer segment absorptance by assuming a visual pigment specific (decadic) absorbance of 0.013 μm^{-1} (rhodopsin, [Turner et al., 2009]) and a rod outer segment length of 39 μm for *S. evermanni* [de Busserolles et al., 2014b] and 45 μm for *M. obtusirostre* as per a similar species (*M. brachygnathum*, [de Busserolles et al., 2014b]). Measurements of ocular media transmittance could not be made from fresh specimens at sea and so were excluded from the modelling.

Results

Description of the yellow pigment

Yellow pigmentation within the retina was noted in ten species of lanternfishes from four different genera all belonging to a single subfamily, the Myctophinae (Table 1). After detailed observation of six species, the distribution of the yellow pigmentation appears to be species-specific, varying in location, shape, size and number of patches (Figure 1*a-f*). Maps of the corrected absorbance at λ_{YPmax} for each species correlate very well with the visual observations and indicate that the pigmentation is restricted to well-

277 defined retinal regions (Figure 1*g-l*). The maximum corrected absorbance at λ_{YPmax} varied
278 between species from 0.78 (*S. evermanni*, Figure 1*j*) to 2.02 (*G. tenuiculus*, Figure 1*g*).
279 Two of the six species analysed showed two patches of yellow pigmentation; *G.*
280 *tenuiculus* possesses two ovoid-like patches, a small one in the dorsal part of the retina
281 and a larger one in the ventral retina (Figure 1*a*), whereas *M. lychnobium* possesses
282 extensive pigment patches covering the entire dorsal part of the retina and the centro-
283 ventral retina arranged in a streak-like pattern (Figure 1*e*). The four other species all
284 possess a single patch of yellow pigmentation. *H. proximum*, *S. rufinus* and *S. evermanni*
285 all have an ovoid-shaped patch situated in the dorsal or dorso-nasal part of the retina
286 (Figure 1*b-d*, respectively), whereas *M. obtusirostre* possesses a streak-like patch in the
287 temporo-ventral area (Figure 1*f*). The density of the yellow pigmentation appears to vary
288 between species with some showing very intense yellow pigmentation (i.e. *G. tenuiculus*,
289 *H. proximum*, *S. rufinus*, *S. evermanni*, Figure 1*a-d*) and others paler pigmentation (i.e.
290 *M. lychnobium*, *M. obtusirostre*, Figure 1*e-f*).
291 Sections through the retina of *G. tenuiculus* reveal that the yellow pigmentation is
292 situated within the outer nuclear layer (Figure 2). The pigmentation appears to be evenly
293 distributed and does not appear to be compartmentalised within any organelles (i.e. oil
294 droplets, ellipsosomes).
295
296 ***Sexual dimorphism***
297 A sexual dimorphism in the size, shape and location of the yellow pigmentation
298 was observed in two species, *M. brachygnathum* and *M. nitidulum*, out of the ten
299 analysed (Figure 3). In *M. brachygnathum* (Figure 3*a*), this sexual dimorphism was

observed in all three females and all three males examined. The females possess a small yellow patch in the central part of the retina just ventral to the optic nerve head. The males possess a larger yellow patch at the periphery of the temporo-ventral retina. In *M. nitidulum* (Figure 3*b*), there also appears to be a sexual dimorphism although this will have to be confirmed as only two females and one male were examined. In the females, the yellow patch takes the shape of a band extending from temporal to ventral retina, located ventral to the optic nerve head. In the male, the patch is approximately circular and located in the nasal periphery. At this stage, it is unknown whether the other eight species with a retinal yellow pigmentation also have a sexual dimorphism as either both sexes were not collected or only immature specimens were available (Table 1).

Spectrophotometry and pigment extraction

Spectrophotometric analysis of the unfixed frozen retinal wholemount of *S. rufinus* revealed that the chemical fixation process had little affect on the absorbance of the yellow pigmentation, with a difference in the λ_{YPmax} between the fresh and fixed samples of only 3 nm and a difference in full width at half maximum of 12 nm (Supplementary Material, Figure S1).

Spectrophotometric analysis of the retinal wholemount of different species revealed that the yellow pigmentation acts as a short-wavelength absorbing (long-pass) filter (Figure 4). The maximum absorbance of the yellow pigmentation (λ_{YPmax}) varies from 356 nm (*M. obtusirostre*, Figure 4*f*) to 443 nm (*G. tenuiculus*, Figure 4*a*). Comparison of the spectral curves, based on the λ_{YPmax} from the different species (Figure 4), suggests that at least three different types of yellow pigments/filters are present with

peak absorbance at approximately 350 nm, 380 nm and 440 nm. In addition, some of these pigments may be present as mixtures. This might be the case for *H. proximum* (Figure 4b), which seems to possess a mixture of the pigment present in *M. obtusirostre* (Figure 4f), *G. tenuiculus* (Figure 4a) and *M. lychnobium* (Figure 4e).

In order to identify the nature of the yellow pigmentation, extraction was attempted from the retinas of two species, *M. aurolaternatum* and *H. proximum*, using water in the former species to extract water-soluble compounds and organic solvents in the latter species to extract carotenoids. However, in each case, the yellow pigment proved to be refractory to extraction, thereby eliminating amino acids, tryptophan derivatives, lipophilic/hydrophilic pigments and carotenoids as the main constituents in the species analysed.

Microspectrophotometry

Microspectrophotometric results for the three species analysed are summarised in Table 2. The mean difference spectra for each type of rod in each species are shown in Figure 5. Except for *M. spinosum*, in which only a single spectral class of rod photoreceptor was identified (492 nm, Figure 5*c*), several spectral classes of rod photoreceptors were found in the two other species.

For *M. obtusirostre*, two classes of rod photoreceptors were identified with mean λ_{max} values of 473 nm in the non-yellow retinal area and 527 nm in the area containing the yellow pigmentation (Figure 5*b*). On the basis of goodness-of-fit to established A_1 and A_2 visual pigment templates [Govardovskii et al., 2000], the pigment in the 473 nm rod was considered to represent 100% A_1 and the pigment in the 527 nm rod was

346 considered to represent 100% A_2. However, given the known relationship between the
347 λ_{max} values of A_1 and A_2 visual pigment pairs [Parry and Bowmaker, 2000], it is very
348 likely that these two pigments originate from two different opsins, since replacement of
349 an A_1 by an A_2 chromophore would only shift the λ_{max} of the 473 nm pigment to 484 nm.

350 For *S. evermanni*, three classes of rod photoreceptor were identified with mean
351 λ_{max} values of 476 nm, 503 nm and 512 nm (Figure 5*c*). While the 476 nm and 503 nm
352 pigments were found to be best-fitted by A_1-based templates, the 512 nm pigment was
353 best-fitted by a template derived from a mixture of 47% A_1 and 53 % A_2. Although both
354 476 nm and 503 nm pigments possess 100% A_1 chromophore thereby indicating the
355 presence of two different opsins, it is unlikely that the 512 nm pigment originates from a
356 third opsin. Most probably, the 512 nm pigment contains the same opsin as the 503 nm
357 pigment, with the difference in wavelength arising from the presence of both A_1 and A_2
358 chromophores within their outer segments.

359

360 ***Molecular analyses***

361 Two opsin transcripts, identified as encoded by two *Rh1* opsin genes, were PCR-
362 amplified from *S. evermanni* retinal cDNA. The sequences were aligned with the *Rh1* rod
363 opsin and representatives of all four cone opsin coding sequences of the zebrafish, *Danio*
364 *rerio*, using Clustal Omega [Sievers et al., 2011]. These alignments were then used to
365 generate Neighbour-Joining and Maximum Likelihood phylogenetic trees
366 (Supplementary Material, Figure S2). In both cases, both *S. evermanni* sequences fall into
367 the same clade as the zebrafish *Rh1* sequences, thereby confirming that both are *Rh1*
368 opsin orthologues. The two sequences were designated as *Rh1-A* and *Rh1-B*.

Rh1-A and *Rh1-B* differ at specific sites that have previously been shown to be important for spectral tuning [Hunt et al., 2001] (Supplementary Material, Figure S3); *Rh1-B* possesses Tyr rather than Phe at site 261 and Ala rather than Ser at site 292. These two substitutions in *Rh1-B* would be expected to result in a long-wavelength shift in the absorbance peak of the pigment compared to *Rh1-A*, and extrapolation from pigments in other species with identical substitutions would indicate a red shift of around 20-25 nm [Hunt et al., 1996; Yokoyama et al., 1995]. This is consistent with the different λ_{max} values found using MSP for rod photoreceptors in this species.

Despite several attempts to complete the sequence of *Rh1-A*, the 5' end remained truncated; the missing portion includes two potential tuning sites (sites 83 and 122). However, since *Rh1A* shows a similar spectral sensitivity to the other myctophid rod opsins (~ 470 nm), which possess Asp83 and Gln122 [Yokoyama et al., 2008], as does *Rh1-B* (the long wave-shifted rod), it is unlikely that either of these sites in *Rh1-A* are substituted.

Rh1-A and *Rh1-B* nucleotide sequences from *S. evermanni* were aligned with all the myctophid *Rh1* opsin sequences available in GenBank, plus the *Rh1* opsin gene nucleotide sequences of the short fin pearleye, *Scopelarchus analis*, the zebrafish, *D. rerio*, the yellow river scaleless carp, *Gymnocypris eckloni*, the elephant shark, *Callorhinchus milii*. The *Rh2* opsin gene nucleotide sequence of *D. rerio* served as an out-group. Neighbour-Joining and Maximum Likelihood analyses were carried out on the aligned nucleotide sequences and the resultant trees (Figure 6) both grouped the *S. evermanni* sequences with those from *Electrona antarctica* and the two *Benthosema* species. The precise location of the *S. evermanni* differed however between the two

methods, with Neighbour-Joining placing the *S. evermanni Rh1-B* sequences subsequent to the evolution of the *Benthosema* genus, whereas Maximum Likelihood placed the *S. evermanni Rh1-B* sequence on a separate branch with the *B. pterotum* sequence only. The relevant bootstrap values are all relatively low, reflecting the overall similarity of the myctophid *Rh1* sequences. It would appear therefore that the *Rh1* duplication in *S. evermanni* arose within the clade defined by three genera, *Symbolophorus*, *Benthosema* and *Electrona*, but its precise location cannot be further verified.

Modelling of the effects of the yellow pigment on photoreceptor spectral sensitivity

Following our observations and measurements using microspectrophotometry in yellow and non-yellow pigmented areas of the retina of *M. obtusirostre*, we concluded that the yellow pigmentation was only associated with the long wave-shifted rod visual pigment and as a result, only modelled this scenario in both species. Species-specific data were used to model the filtering effect of the yellow pigment on the photoreceptor spectral sensitivity (i.e. species-specific rod outer segment spectral absorptance and species-specific yellow pigment spectral transmittance).

Results show that the yellow filter decreases the absolute sensitivity at the peak of the longwave-shifted rod visual pigment, shifts the overall sensitivity peak slightly toward longer wavelengths, and narrows the spectral sensitivity function by absorbing strongly at short wavelengths (Figures 7, 8). In *M. obtusirostre*, the yellow pigment narrows the full-width at half-maximum (FWHM) bandwidth of the long wave-shifted visual pigment from 248 nm to 142 nm (Figure 7) and shifts the peak of maximum absorbance of the rods 6 nm toward longer wavelengths.

In contrast to *M. obtusirostre*, two long wave-shifted rod visual pigments were found in *S. evermanni* (Figure 8*a*). However, it is unknown if the yellow pigment is associated with both longwave-shifted visual pigments or only one of the two. As a consequence, three different scenarios were modelled (Figure 8*b*-*d*). For the 503 nm visual pigment, the FWHM of the rods would decrease from 125 nm to 93 nm with the addition of the yellow pigment, while for the 512 nm visual pigment, the FWHM would decrease from 149 nm to 108 nm. In terms of the wavelength of maximum absorbance of the rod spectral sensitivity function, a slight shift toward longer wavelengths would be predicted with the addition of the yellow pigment (10 nm shift for rods containing the 503 nm pigment and an 8 nm shift for the 512 nm pigment). Depending on the scenario, *S. evermanni* could possess rods with peaks of quantal spectral sensitivity at 476 nm, 513 nm and 520 nm if both of the long wave-shifted visual pigments are associated with the yellow pigment (Figure 8*b*), or at 476 nm, 513 nm and 512 nm (Figure 8*c*) or 476 nm, 503 nm and 520 nm (Figure 8*d*) if only one or the other of the long wave-shifted visual pigments is associated with the yellow pigment.

Discussion

The unique yellow pigment in the retina of myctophids

In this study, we describe a novel visual specialisation, a photostable yellow pigmentation, present in the retina of several species of lanternfishes. Retinal photostable yellow pigmentation has previously been observed in a number of animals including species of lamprey [Collin et al., 2003] and lungfish [Bailes et al., 2006], the ornate dragon lizard [Barbour et al., 2002], and Amazonian cichlid fishes [Muntz, 1973].

However, in contrast to these other animals, the yellow pigmentation in lanternfishes is restricted to well-defined areas (patches) of the retina, which appear to be species-specific in terms of the number, size, location and pigment density. Moreover, the location of the yellow pigmentation throughout the outer nuclear layer of the retina of myctophids differs from what has been previously observed in other species, where it is found within the distal region of the inner segment and/or diffusely distributed within the myoid region of the photoreceptors [Barbour et al., 2002; Collin et al., 2003; Bailes et al., 2006].

Unfortunately, the composition of the yellow pigmentation in myctophids could not be identified in this study. Coloration in animals is primarily due to the presence of melanins and carotenoids, although other types of pigment have been shown to be responsible for animal coloration i.e. porphyrins, pterins, flavins, psittacofulvins, [McGraw, 2006] and amino acids [Thorpe et al., 1993]. Specifically, yellow pigmentation in ocular tissues has been identified as carotenoids (in pufferfish cornea [Appleby and Muntz, 1979], in avian retinal oil droplets [Goldsmith et al., 1984], in the human macula [Bone et al., 1985]), as tryptophan derivatives (in the lens of terrestrial vertebrates [van Heyningen, 1971a, b], in the lenses of deep-sea fishes [Thorpe et al., 1992]) and as mycosporine-like amino acids (in the lenses of deep-sea fishes [Thorpe et al., 1993]). Results from our study seem to exclude all of these compounds, plus lipophilic or hydrophilic pigments (e.g. porphyrins and psittacofulvins) since water and non-polar solvents were also unsuccessful. However, extraction was only performed in two species: *M. aurolaternatum* for which no spectrum is available, and *H. proximum*. Since no carotenoids were extracted in *H. proximum*, the pigment present in *H. proximum* and the

two other species with similar spectra, *M. lychnobium* and *M. obtusirostre*, may therefore not be carotenoid based, unless bond in such a way that does not allow extraction with standard methods. The spectra obtained for the pigment in the remaining three species, *G. tenuiculus*, *S. evermanni* and *S. rufinus*, are however different, with two peaks that are broadly similar to spectra obtained from carotenoids [Goldsmith et al., 1984]. So although it would seem unlikely that the pigmentation has a different basis between species, this cannot be ruled out. Further analyses will have to be conducted to confirm the presence/absence of these compounds in all species and investigate other possibilities.

Melanins are often implicated in animal coloration and provide the black pigmentation of the retinal pigment epithelium. They exist however in two distinct forms, brown to black eumelanin and yellow to red pheomelanin. Melanin is also known to be difficult to extract from tissues due to its heterogeneous nature, and its association with proteins [Taft, 1949; Liu et al., 2003]. Therefore, the difficulty in extracting the lanternfish yellow pigment could be consistent with the presence of a melanin and its colour would indicate that it is composed of pheomelanin. Although pheomelanin has yet to be directly observed in fishes [Ito and Wakamatsu, 2003], the presence of agouti signalling proteins (ASIP), which control the production of pheomelanin, in several fishes i.e goldfish [Cerda-Reverter et al., 2005], zebrafish and several species of pufferfishes [Klovins and Schiöth, 2005] indicates that it may be present; it could therefore be one of the components of the yellow pigmentation in lanternfishes.

Another unique feature of the yellow pigmentation in lanternfishes is its sexual dimorphism, observed so far in two species of the genus *Myctophum*. Although sexual dimorphism in the visual system has already been observed in insects (houseflies

[Franceschini et al., 1981; Zeil, 1983], march flies [Hornstein et al., 2000], moths [Meyer-Rochow and Lau, 2008], butterflies [Arikawa et al., 2005; Sison-Mangus et al., 2006]), crustaceans (copepods [Land, 1984, 1988] and primates [Hunt, 2005], to our knowledge, this is the first observation of sexual dimorphism in the visual system of any non-primate vertebrate. Within these examples, sexual dimorphism in the visual system has been observed at several levels, eye morphology (flies [Franceschini et al., 1981; Zeil, 1983]), retinal organisation (flies [Zeil, 1983; Hornstein et al., 2000]), and spectral sensitivity (butterflies [Arikawa et al., 2005; Sison-Mangus et al., 2006], primates (Hunt et al., 2005]). Lanternfishes show a new type of sexual dimorphism in the visual system, functionally similar to the visual system of the small white butterfly, *Pieris rapae crucivora* [Arikawa et al., 2005], where a filter is present in the ommatidia, which tunes visual sensitivity. However, in contrast to the small white butterfly, both male and female lanternfishes possess the filter but in different areas of the retina.

Visual pigments and spectral tuning in myctophids

The presence of different spectral classes of the rod photoreceptors in two lanternfish species with yellow retinal pigmentation indicate the presence of more than one visual pigment. While most lanternfish species possess a single photoreceptor class [Turner et al., 2009], two photoreceptor classes have been observed in four other species, *Ceratoscopelus warmingii* [Douglas et al., 2003], *H. proximum, M. aurolaternatum* [Turner et al., 2009] and *M. nitidulum* [Hasegawa et al., 2008], with the last three species all possessing yellow pigmentation (this study). Based on the conclusions of this study and known relationships between the λ_{max} values of A_1 and A_2 visual pigment pairs

507 [Parry and Bowmaker, 2000], the presence of two different opsins can be predicted for *H.*
508 *proximum*, *M. nitidulum*, [Hasegawa et al., 2008; Turner et al., 2009], *M. obtusirostre* and
509 *S. evermanni*. This was confirmed at the molecular level for *S. evermanni* (this study).
510 A pure rod retina with a single *Rh1* pigment is typical among deep-sea fishes
511 [Hunt et al., 2001]. However, analysis of the rod opsin coding sequences expressed in *S.*
512 *evermanni* revealed the presence of two *Rh1* opsin genes (*Rh1-A* and *Rh1-B*). This is only
513 the second case of a rod opsin duplication recorded for a deep-sea fish, the first being the
514 pearleye *Scopelarchus analis* [Pointer et al., 2007]. However, in contrast to *S. analis* for
515 which the duplication of *Rh1* results in two spectrally similar visual pigments (486 nm
516 and 479 nm, [Pointer et al., 2007]), the duplication in *S. evermanni* gives rise to two
517 spectrally distinct visual pigments, with peaks at 476 nm and 503 nm. Moreover, while
518 the two *Rh1* genes are phylogenetically different in *S. analis*, indicating an early
519 duplication in evolutionary history [Pointer et al., 2007], the *Rh1-A* and *Rh1-B* genes in *S.*
520 *evermanni* are phylogenetically very similar, indicating the origin of the duplication
521 within a clade defined by three genera of myctophids. The fact that this duplication
522 appeared at a specific stage in the evolutionary history of the family, and is only present
523 in the Myctophinae subfamily, could explain why it has not been reported previously.
524 *Rh1* gene duplications have only been reported in teleost fishes and even then, are
525 quite rare. In addition to the two deep-sea species mentioned above, it has been observed
526 in the cyprinid zebrafish *D. rerio* [Morrow et al., 2011] and a few eel species [Hunt et al.,
527 2013]. The expression of the second *Rh1* gene in the eel is associated with a change in the
528 spectral conditions of their habitat [Archer et al., 1995]. Myctophids show marked
529 differences in habitat depending on their developmental stage, with larvae inhabiting the

well-lit surface layers of the ocean [Sabates et al., 2003] and juvenile and adults occupying the deeper mesopelagic zone. Moreover, larvae and juvenile/adults also possess different types of photoreceptors, the larvae having both rods and cones [Bozzano et al., 2007], while juveniles/adults possess only rods. There is therefore a change in visual pigment expression between larval and juvenile/adult stage myctophids. However, microspectrophotometric results predict that both *Rh1* genes are expressed in the retina of the adult lanternfish, although, it is unknown at this stage if both genes are also expressed in the larvae. While most deep-sea organisms produce bioluminescent emission in the blue-green region of the visible spectrum, several organisms do produce longer wavelength signals [Widder, 2010], the most extreme case being the red-bioluminescence produced by some stomiid dragonfishes [Widder et al., 1984]. Some of these far-red illuminating fishes are known to prey on myctophids [Sutton and Hopkins, 1996] and the long wave-shifted visual pigment in some of these lanternfishes (i.e. *M. nitidulum* and *M. obtusirostre*) could potentially have evolved as a mechanism to detect these predators [Hasegawa et al., 2008; Turner et al., 2009].

Putative functions of the yellow pigment in myctophids

Intraocular filters are thought to have many functions in vertebrates. In well lit environments, they may improve visual acuity by reducing chromatic aberration and scatter (yellow lens and cornea, [Walls, 1931; Walls and Judd, 1933; Muntz, 1973; Barbour et al., 2002]), enhance the discrimination of colours by narrowing the spectral sensitivity of the visual pigment (i.e. oil droplets, [Hart, 2001]), filter out the potentially damaging short-wavelengths present in bright environments [Collin et al., 2003], or allow

553 the detection of fluorescent light emitted by certain organisms [Sparks et al., 2014]. In the
554 deep-sea, only two types of intraocular filters have been observed previously in teleosts:
555 yellow lenses [Douglas and Thorpe, 1992] and the yellow pigmentation of the retina
556 found in myctophids. In the mesopelagic zone, yellow lenses may increase hue
557 discrimination in order to better visualise bioluminescent flashes or to break down the
558 counterilluminating camouflage of other species [Muntz, 1976; Somiya, 1976; 1982,
559 Douglas and Thorpe, 1992]. Indeed, during the day in the mesopelagic zone, the
560 simultaneous presence of downwelling sunlight and bioluminescent flashes might render
561 the detection of both signals difficult. More particularly, the presence of downwelling
562 sunlight might reduce the contrast, and thereby the visibility, of bioluminescent
563 emissions, which could be detrimental in terms of survival. However, since most
564 bioluminescent emissions have a broader spectrum than downwelling light [Herring,
565 1983], yellow lenses might prevent this problem by cutting off most of the background
566 illumination, thereby accentuating the signal. Lanternfish species with a yellow retinal
567 pigmentation are found at very different depths during the day [de Busserolles et al.,
568 2013]. However, at night they all migrate towards the surface to depths of <4 m [de
569 Busserolles et al., 2013], where downwelling light produced by the moon and stars
570 [Johnsen et al., 2004] may reduce the visibility of bioluminescent emissions. Therefore,
571 in a similar way to yellow lenses, the presence of retinal yellow pigmentation could
572 enhance the contrast of bioluminescent emissions against the night downwelling light in
573 specific regions of the visual field.

574 Another potential function or outcome of yellow filtering in the mesopelagic
575 realm is to increase the contrast of fluorescent objects such as siphonophores and other

576 gelatinous zooplankton, which constitute regular prey [Kinzer and Schulz, 1985; Hopkins
577 and Gartner, 1992; Beamish et al., 1999] and potential predators [Haddock et al., 2005;
578 Pagès and Madin, 2010] of myctophids. Three areas of evidence support this idea. Firstly,
579 several studies have shown that a number of mesopelagic animals both bioluminesce and
580 fluoresce [Haddock et al., 2005; Haddock et al., 2010; Widder, 2010]. Secondly, the light
581 distribution in the mesopelagic zone, peaking around 475nm (downwelling light and
582 bioluminescence, [Widder, 2010]), is well matched to the excitation wavelengths needed
583 to trigger a variety of fluorescent marine compounds [Mazel et al., 2004; Haddock et al.,
584 2005; Alieva et al., 2008; Vogt et al., 2008] and this means that, at the right depth and
585 resulting light level, fluorescence may be a significant component of the signals from
586 such animals. Thirdly, as the new wave of photographers interested in capturing
587 fluorescence are aware [Mazel, 2005; www.nightsea.com], a yellow blocking filter
588 enhances the contrast at longer wavelengths for yellow, orange or red emissions of
589 fluorescence [Sparks et al., 2014]. This is because yellow removes the wash of blue
590 excitation and leaves only the glowing fluorescent emission component, a highly
591 contrasting signal, especially in dim illumination. As a result, in addition to possibly
592 enhancing bioluminescent contrast, the yellow filters in the eyes of myctophids may also
593 enable them to see fluorescent gelatinous prey and/or predators and any other fluorescent
594 signals at depth.

595 Different species of lanternfishes possess different yellow pigmented areas in the
596 retina that may serve to enhance sensitivity to bioluminescence and/or fluorescence in
597 different parts of the visual field. This implies interspecific differences in behaviour.
598 Myctophids show a variety of interspecific differences in behaviour with respect to their

depth distribution [Karnella, 1987], migration pattern [Watanabe et al., 1999] and diet [Kozlov, 1995; Shreeve et al., 2009; Van Noord et al., 2013]. Since all the species which possess a retinal yellow pigmentation vertically migrate to the surface at night, interspecific differences in the location of the yellow pigmentation could potentially reflect differences in diet, a consequence of different nutritional requirements, niche partitioning and/or body size differences between males and females [Shine, 1989]. Unfortunately, data on diet are quite limited for lanternfishes and highly variable between seasons and geographic regions [Kozlov, 1995], making any diet/vision comparison impossible at this stage. Moreover, no studies have been conducted on possible diet differences between sexes, which would potentially explain the observed sexual dimorphism in the retinal yellow pigmentation. Sexual dimorphism in food choices has been reported in a number of organisms, as a consequence of different nutritional requirements, food competition, habitat and body size between males and females [Shine, 1989]. Sexual dimorphism in size has been observed in several lanternfish species [Gartner, 1993; Braga et al., 2008; Flynn and Paxton, 2012] and some differences in distribution between sexes have been suggested [Flynn and Paxton, 2012], supporting the possible role of the retinal yellow pigmentation in food choice.

The sexual dimorphism in the retinal yellow pigment implies a possible role in intraspecific/sexual communication. All the species possessing the yellow pigment are also sexually dimorphic in the location and size of their caudal luminous organs, with all males possessing a large supracaudal organ and all females possessing a smaller infracaudal organ [Herring, 2007]. If the retinal yellow pigmentation is involved in sexual communication, interspecific differences in the shape, size and location of the retinal

622 pigment patches could be associated with differences in luminous organ location, size
623 and shape between species, taking into consideration the position of the fish in the water
624 column. Unfortunately, this information is not available for the species analysed and it is
625 unknown how males and females position themselves with respect to one another in the
626 water column. Further analyses of the retinal yellow pigmentation in both sexes, at
627 several different life stages and from all the species possessing this yellow pigment will
628 shed more light on the function and development of this new visual specialisation.

629 Overall, our findings indicate an evolutionary pressure to visualise
630 prey/predators/mates in a specific part of each species' visual field. Our results also add a
631 new dimension to the contribution made by recent studies [Davis et al., 2014; Kenaley et
632 al., 2014] on the evolutionary history in the deep-sea by identifying a visual "arms race",
633 in term of visual adaptation, between lanternfishes and dragonfishes. In fact, while
634 dragonfishes have evolved a secret communication/predation channel by using red
635 bioluminescence, lanternfishes, by virtue of their visual sexual dimorphism, are taking
636 the race a step further by inviting "sex in the blue-light district of the deep-sea". It
637 appears we are yet to unlock all of the secrets of bioluminescent communication in the
638 deep-sea.

639

640 ## Acknowledgments

641 We wish to thank Dr. Mike Hall (AIMS) and the Masters and crews of the RV *Cape*
642 *Ferguson* for sea time and sampling opportunities. We gratefully acknowledge John
643 Denton and the American Museum of Natural History, New York, USA for providing the
644 additional *M. brachygnathum* specimen and John Paxton (Australian Museum) for

providing most of the fish identification. We thank Prof. Julian Partridge (University of Bristol) for helpful discussions regarding the yellow pigment absorption spectra and Eduardo Garza-Gisholt for his help in using his R script for the creation of the yellow pigment maps. This work was supported by grants to SPC, NSH, DMH and NJM (DP110103294 and LP0775179) from the Australian Research Council and the West Australian State Government. WID is supported by the Australian Research Council (FT110100176 and DP140102117). FdB was supported by a Scholarship for International Research Fees and a University International Stipend at the University of Western Australia.

References

Alieva NO, Konzen KA, Field SF, Meleshkevitch EA, Hunt ME, Beltran-Ramirez V, Miller DJ, Wiedenmann J, Salih A, Matz MV (2008): Diversity and evolution of coral fluorescent proteins. PLoS ONE 3(7): e2680. doi:10.1371/journal.pone.0002680.

Appleby SJ, Muntz WRA (1979): Occlusable yellow corneas in Tetraodontidae. J Exp Biol 83(1):249-259.

Archer S, Hope A, Partridge JC (1995): The Molecular Basis for the Green-Blue Sensitivity Shift in the Rod Visual Pigments of the European Eel. Proc R Soc Lond B 262:289-295.

Arikawa K, Wakakuwa M, Qiu X, Kurasawa M, Stavenga DG (2005): Sexual dimorphism of short-wavelength photoreceptors in the small white butterfly, *Pieris rapae crucivora*. J Neurosci 25:5935-5942.

Baddeley A, Turner R (2005): Spatstat: an R package for analyzing spatial point patterns. J Stat Softw 12:1-42.

Bailes HJ, Robinson SR, Trezise AEO, Collin SP (2006): Morphology, characterization, and distribution of retinal photoreceptors in the Australian lungfish *Neoceratodus forsteri* (Krefft, 1870). J Comp Neurol 494:381-397.

Bailes HJ, Davies WL, Trezise AEO, Collin SP (2007): Visual pigments in a living fossil, the Australian lungfish *Neoceratodus forsteri*. BMC Evol Biol 7(200). doi:10.1186/1471-2148-7-200.

Barbour HR, Archer MA, Hart NS, Thomas N, Dunlop SA, Beazley LD, Shand J (2002): Retinal characteristics of the ornate dragon lizard, Ctenophorus ornatus. J Comp Neurol 450:334-344.

Beamish RJ, Leask KD, Ivanov OA, Balanov AA, Orlov AM, Sinclair B (1999): The ecology, distribution, and abundance of midwater fishes of the Subarctic Pacific gyres. Prog Oceanogr 43:399-442.

Bone RA, Landrum JT, Tarsis SL (1985): Preliminary identification of the human macular pigment. Vision Res 25(11):1531-1535.

Bowmaker JK, Hunt DM (2006): Evolution of vertebrate visual pigments. Curr Biol 16:484-489.

Bowmaker JK (2008): Evolution of vertebrate visual pigments. Vision Res 48:2022-2041.

Bozzano A, Pankhurst PM, Sabatés A (2007): Early development of eye and retina in lanternfish larvae. Vis Neurosci 24:423-436.

Braga AC, Costa PAS, Nunan GW (2008): First record of the firebrow lanternfish Diaphus adenomus (Myctophiformes : Myctophidae) from the South Atlantic. J Fish Biol 73: 296-301.

Cerda-Reverter JM, Haitina T, Schioth HB, Peter RE (2005): Gene structure of the goldfish agouti-signaling protein: a putative role in the dorsal-ventral pigment pattern of fish. Endocrinology 146(3):1597-1610.

Coimbra JP, Marceliano MLV, Andrade-da-Costa BLS, Yamada ES (2006): The retina of tyrant flycatchers: topographic organization of neuronal density and size in the ganglion cell layer of the Great Kiskadee *Pitangus sulphuratus* and the Rusty Margined Flycatcher *Myiozetetes cayanensis* (Aves: Tyrannidae). Brain Behav Evol 68:15-25.

Collin SP, Hart NS, Shand J, Potter IC (2003): Morphology and spectral absorption characteristics of retinal photoreceptors in the southern hemisphere lamprey (*Geotria australis*). Vis Neurosci 20:119-130.

Crescitelli F (1990): Adaptations of visual pigments to the photic environment of the deep sea. J Exp Zool 256:66-75.

Davies WL, Collin SP, Hunt DM (2012): Molecular ecology and adaptation of visual photopigments in craniates. Mol Ecol 21:3121-3158.

Davies WL, Cowing JA, Bowmaker JK, Carvalho LS, Gower DJ, Hunt DM (2009): Shedding light on serpent sight: the visual pigments of henophidian snakes. J neurosci 29:7519-7525.

Davis MP, Holcroft NI, Wiley EO, Sparks JS, Smith WL (2014): Species-specific bioluminescence facilitates speciation in the deep sea. Mar Biol 161:1139-1148.

de Busserolles F, Fitzpatrick JL, Paxton JR, Marshall NJ, Collin SP (2013): Eye-size variability in deep-sea lanternfishes (Myctophidae): an ecological and phylogenetic study. PLoS One 8(3): e58519. doi:10.1371/journal.pone.0058519.

de Busserolles F, Marshall NJ, Collin SP (2014a): The eyes of lanternfishes (Myctophidae, teleostei): novel ocular specializations for vision in dim light. J Comp Neurol 522:1618–1640.

de Busserolles F, Fitzpatrick JL, Marshall NJ, Collin SP (2014b) The influence of photoreceptor size and distribution on optical sensitivity in the eyes of lanternfishes (Myctophidae). PLoS ONE 9(6): e99957. doi:10.1371/journal.pone.0099957.

Douglas RH, Thorpe A (1992): Short-wave absorbing pigments in the ocular lenses of deep-sea teleosts. J Mar Biol Ass UK 72:93-112.

726 Douglas RH, Partridge JC (1997): On the visual pigments of deep-sea fish. J Fish Biol
727 50:68-85.
728 Douglas RH, Hunt DM, Bowmaker JK (2003): Spectral sensitivity tuning in the deep-sea.
729 In: Sensory Processing in Aquatic Environments (Collin SP, Marshall J, eds), pp
730 323-342: Springer.
731 Flynn AJ, Paxton JR (2012): Spawning aggregation of the lanternfish *Diaphus danae*
732 (family Myctophidae) in the north-western Coral Sea and associations with tuna
733 aggregations. Mar Freshw Res 63: 1255-1271.
734 Franceschini N, Hardie R, Ribi W, Kirschfeld K (1981): Sexual dimorphism in a
735 photoreceptor. Nature 291:241-244.
736 Gartner JV (1993): Patterns of reproduction in the dominant lanternfish species (Pisces:
737 Myctophidae) of the eastern Gulf of Mexico, with a review of reproduction
738 among tropical-subtropical Myctophidae. Bull Mar Sci 52: 721-750.
739 Garza Gisholt E, Hemmi JM, Hart NS, Collin SP (2014): A comparison of spatial
740 analysis methods for the construction of topographic maps of retinal cell density.
741 PLoS ONE 9(4): e93485. doi:10.1371/journal.pone.0093485.
742 Goldsmith TH, Collins JS, Licht S (1984): The cone oil droplets of avian retinas. Vision
743 Res 24(11):1661-1671.
744 Govardovskii VI, Fyhrquist N, Reuter T, Kuzmin DG, Donner K (2000): In search of the
745 visual pigment template. Vis Neurosci 17:509-528.
746 Haddock SHD, Dunn CW, Pugh PR, Schnitzler CE (2005): Bioluminescent and red-
747 fluorescent lures in a deep-sea siphonophore. Science 309:263.
748 Haddock SHD, Moline MA, Case JF (2010): Bioluminescence in the sea. Ann Rev Mar
749 Sci 2:443-493.
750 Hart N, Partridge J, Cuthill I (1998): Visual pigments, oil droplets and cone
751 photoreceptor distribution in the european starling (*Sturnus vulgaris*). J Exp Biol
752 201:1433-1446.
753 Hart NS (2001): The Visual Ecology of Avian Photoreceptors. Prog Retinal Eye Res
754 20:675-703.
755 Hart NS (2002): Vision in the peafowl (Aves: *Pavo cristatus*). J Exp Biol 205:3925-3935.
756 Hart NS, Lisney TJ, Marshall NJ, Collin SP (2004): Multiple cone visual pigments and
757 the potential for trichromatic colour vision in two species of elasmobranch. The
758 Journal of Experimental Biology 207:4587-4594.
759 Hart NS, Theiss SM, Harahush BK, Collin SP (2011) Microspectrophotometric evidence
760 for cone monochromacy in sharks. Naturwissenschaften 98:193-201.
761 Hart NS, Coimbra JP, Collin SP, Westhoff G (2012) Photoreceptor types, visual
762 pigments, and topographic specializations in the retinas of hydrophiid sea snakes.
763 J Comp Neurol 520:1246-1261.
764 Hasegawa EI, Sawada K, Abe K, Watanabe K, Uchikawa K, Okazaki K, Toyama M,
765 Douglas RH (2008): The visual pigments of a deep-sea myctophid fish
766 *Myctophum nitidulum* Garman; an HPLC and spectroscopic description of a non-
767 paired rhodopsin–porphyropsin system. J Fish Biol 72:937-945.
768 Herring PJ (1983): The spectral characteristics of luminous marine organisms. Proc R
769 Soc Lond B 220:183-217.
770 Herring PJ (2007): Sex with the lights on? A review of bioluminescent sexual
771 dimorphism in the sea. J Mar Biol Ass UK 87:829-842.

Hopkins TL, Gartner JV, Jr. (1992): Resource-partitioning and predation impact of a low-latitude myctophid community. Mar Biol 114:185-197.
Hornstein EP, O'Carroll DC, Anderson JC, Laughlin SB (2000): Sexual dimorphism matches photoreceptor performance to behavioural requirements. Proc R Soc Lond B 267:2111-2117.
Hunt DM, Fitzgibbon J, Slobodyanyuk SJ, Bowmakers JK (1996): Spectral tuning and molecular evolution of rod visual pigments in the species flock of cottoid fish in Lake Baikal. Vision Res 36:1217-1224.
Hunt DM, Dulai KS, Partridge JC, Cottrill P, Bowmaker JK (2001): The molecular basis for spectral tuning of rod visual pigments in deep-sea fish. J Exp Biol 204:3333-3344.
Hunt DM, Jacobs GH, Bowmaker JK (2005): The genetics of primate visual pigments. In: The primate visual system: a comparative approach (Kremers J, ed): John Wiley & Sons, Ltd, Chichester.
Hunt DM, Hart NS, Collin SP (2013): Sensory systems. In: Eel physiology (Trischitta F, Takei Y, Sebert P, eds), pp 118-159. New York: CRC Press.
Ito S, Wakamatsu K (2003): Quantitative analysis of eumelanin and pheomelanin in humans, mice, and other animals: a comparative review. Pigment Cell Res 16(5):523-531.
Johnsen S, Widder EA, Mobley CD (2004): Propagation and perception of bioluminescence: factors affecting counterillumination as a cryptic strategy. Biol Bull 207:1-16.
Karnella C (1987): Family Myctophidae, lanternfishes. In: Gibbs RH, Krueger WH (eds) Biology of midwater fishes of the bermuda Ocean Acre, pp 51-168. Washington, D.C.: Smithsonian Institution Press.
Kenaley CP, DeVaney SC, Fjeran TT (2014): The complex evolutionary history of seeing red: molecular phylogeny and the evolution of an adaptive visual system in deep-sea dragonfishes (Stomiiformes: Stomiidae). Evolution 68(4):996-1013.
Kinzer J, Schulz K (1985): Vertical distribution and feeding patterns of midwater fish in the central equatorial Atlantic. I. Myctophidae. Mar Biol 85:313-322.
Klovins J, Schiöth HB (2005): Agouti-related proteins (AGRPs) and agouti-signaling peptide (ASIP) in fish and chicken. Ann N Y Acad Sci 1040(1):363-367.
Kozlov AN (1995): A review of the trophic role of mesopelagic fish of the family Myctophidae in the Southern Ocean ecosystem. CCAMLR Science 2:71-77.
Land MF (1984): Crustacea. In: Photoreception and vision in invertebrates (Ali MA, ed), pp 401-438.
Land MF (1988): The functions of eye and body movements in *Labidocera* and other copepods. J Exp Biol 140:381-391.
Levine JS, MacNichol Jr EF (1985): Microspectrophotometry of primate photoreceptors: art, artefact and analysis. In: The visual system (Fein A, Levine Js, eds), pp 73-87. New York: Liss.
Liu Y, Kempf VR, Brian Nofsinger J, Weinert EE, Rudnicki M, Wakamatsu K, Ito S, Simon JD (2003): Comparison of the structural and physical properties of human hair eumelanin following enzymatic or acid/base extraction. Pigment Cell Res 16(4):355-365.

817 Lythgoe J, Partridge J (1989): Visual pigments and the acquisition of visual information.
818 J Exp Biol 146:1-20.
819 McGraw KJ (2006): Mechanics of uncommon colors: pterins, porphyrins and
820 psittacofulvins. In: Bird Coloration: Mechanism and Measurement (Hill GE,
821 McGraw KJ, eds), pp 354-398. Harvard University Press.
822 MacNichol Jr EF (1986): A unifying presentation of photopigment spectra. Vision Res
823 26:1543-1556.
824 Mazel CH, Cronin TW, Caldwell RL, Marshall NJ (2004): Fluorescent enhancement of
825 signaling in a mantis shrimp. Science 303:51.
826 Mazel CH (2005): Underwater fluorescence photography in the presence of ambient
827 light. Limnol Oceanogr 3:499-510.
828 Meyer-Rochow VB, Lau TF (2008): Sexual dimorphism in the compound eye of the
829 moth *Operophtera brumata* (Lepidoptera, Geometridae). Invert Biol 127:201-216.
830 Morrow JM, Lazic S, Chang BSW (2011): A novel rhodopsin-like gene expressed in
831 zebrafish retina. Vis Neurosci 28:325-335.
832 Muntz W (1976): On yellow lenses in mesopelagic animals. J Mar Biol Assoc UK
833 56:963-976.
834 Muntz WRA (1973): Yellow filters and the absorption of light by the visual pigments of
835 some amazonian fishes. Vision Res 13:2235-2254.
836 Pagès F, Madin LP (2010): Siphonophores eat fish larger than their stomachs. Deep Sea
837 Res II 57:2248-2250.
838 Parry JWL, Bowmaker JK (2000): Visual pigment reconstitution in intact goldfish retina
839 using synthetic retinaldehyde isomers. Vision Res 40:2241-2247.
840 Partridge JC, Archer SN, Vanoostrum J (1992): Single and multiple visual pigments in
841 deep-sea fishes. J Mar Biol Ass UK 72:113-130.
842 Pointer MA, Carvalho LS, Cowing JA, Bowmaker JK, Hunt DM (2007): The visual
843 pigments of a deep-sea teleost, the pearl eye *Scopelarchus analis*. J Exp Biol
844 210:2829-2835.
845 Sabates A, Bozzano A, Vallvey I (2003): Feeding pattern and the visual light
846 environment in myctophid fish larvae. J Fish Biol 63:1476-1490.
847 Saitou N, Nei M (1987): The neighbor-joining method: a new method for reconstructing
848 phylogenetic trees. Mol Biol Evol 4:406-425.
849 Sedmak JJ, Weerasinghe D, Jolly S (1990): Extraction and quantitation of astaxanthin
850 from *Phaffia rhodozyma*. Biotechnol Tech 4 (2), 107-112.
851 Shine R (1989): Ecological causes for the evolution of sexual dimorphism: a review of
852 the evidence. Quart Rev Biol 64:419-461.
853 Shreeve RS, Collins MA, Tarling GA, Main CE, Ward P, Johnston NM (2009): Feeding
854 ecology of myctophid fishes in the northern Scotia Sea. Mar Ecol Prog Ser
855 386:221-236.
856 Siebeck UE, Collin SP, Ghoddusi M, Marshall NJ (2003): Occlusable corneas in
857 toadfishes: light transmission, movement and ultrastruture of pigment during
858 light- and dark-adaptation. J Exp Biol 206(13):2177-2190.
859 Sievers F, Wilm A, Dineen D, Gibson TJ, Karplus K, Li W, Lopez R, McWilliam H,
860 Remmert M, Soding J, Thompson JD, Higgins DG (2011): Fast, scalable
861 generation of high-quality protein multiple sequence alignments using Clustal
862 Omega. Mol Syst Biol 7:539.

Sison-Mangus MP, Bernard GD, Lampel J, Briscoe AD (2006): Beauty in the eye of the beholder: the two blue opsins of lycaenid butterflies and the opsin gene-driven evolution of sexually dimorphic eyes. J Exp Biol 209:3079-3090.

Somiya H (1976): Functional significance of the yellow lens in the eyes of *Argyropelecus affinis*. Mar Biol 34:93-99.

Somiya H (1982): `Yellow Lens' Eyes of a Stomiatoid Deep-Sea Fish, *Malacosteus niger*. Proc R Soc Lond B 215:481-489.

Sparks JS, Schelly RC, Smith WL, Davis MP, Tchernov D, Pieribone VA, Gruber DF (2014): The covert world of fish biofluorescence: a phylogenetically widespread and phenotypically variable phenomenon. PLoS One 9:e83259.

Stone J (1981): The whole mount handbook: a guide to the preparation and analysis of retinal whole mounts. Sydney: Maitland Publications. 128 p.

Sutton TT, Hopkins TL (1996): Trophic ecology of the stomiid (Pisces: Stomiidae) fish assemblage of the eastern Gulf of Mexico: Strategies, selectivity and impact of a top mesopelagic predator group. Mar Biol 127:179-192.

Taft EB (1949): Melanin solubility in tissue sections. Nature 164:1133-1134.

Tamura K, Stecher G, Peterson D, Kumar S (2013): MEGA6: Molecular Evolutionary Genetics Analysis (MEGA) software version 6.0. Mol Biol Evol 30 2725-2729.

Temple S, Hart NS, Marshall NJ, Collin SP (2010): A spitting image: specializations in archerfish eyes for vision at the interface between air and water. Proc R Soc B 277:2607-2615.

Thorpe A, Truscott RJW, Douglas RH (1992): Kynurenine identified as the short-wave absorbing lens pigment in the deep-sea fish *Stylephorus chordatus*. Exp Eye Res 55(1):53-57.

Thorpe A, Douglas RH, Truscott RJW (1993): Spectral transmission and short-wave absorbing pigments in the fish lens - I. Phylogenetic distribution and identity. Vision Res 33(3):289-300.

Toomey MB, McGraw KJ (2007): Modified saponification and HPLC methods for analyzing carotenoids from the retina of quail: implications for its use as a nonprimate model species. Invest Ophthalmol Vis Sci 48 (9), 3976-3982.

Toomey MB, McGraw KJ (2009): Seasonal, sexual, and quality related variation in retinal carotenoid accumulation in the house finch (*Carpodacus mexicanus*). Funct Ecol 23 (2), 321-329.

Truscott RJW, Carver JA, Thorpe A, Douglas RH (1992): The identification of 3-hydroxykynurenine as the lens pigment in he gourami Trichogaster trichopterus. Exp Eye Res 54: 1015-1017.

Turner JR, White EM, Collins MA, Partridge JC, Douglas RH (2009): Vision in lanternfish (Myctophidae): Adaptations for viewing bioluminescence in the deep-sea. Deep Sea Res I 56:1003-1017.

Ullmann JFP, Moore BA, Temple SE, Fernandez-Juricic E, Collin SP (2011): The retinal wholemount technique: a window to understanding the brain and behaviour. Brain Behav Evol 79: 26-44.

van Heyningen R (1971a): Fluorescent glucoside in the human lens. Nature 230:393-394.

van Heyningen R (1971b): Fluorescent derivatives of 3-hydroxy-L-kynurenine in the lens of man, the baboon, and the grey squirrel. Biochem J 123:30-31.

Van Noord JE, Olson RJ, Redfern JV, Kaufmann RS (2013): Diet and prey selectivity in three surface-migrating myctophids in the eastern tropical Pacific. Ichthyol Res 60:287-290.

Vogt A, D'Angelo C, Oswald F, Denzel A, Mazel CH, Matz MV, Ivanchenko S, Nienhaus GU, Wiedenmann J (2008): A green fluorescent protein with photoswitchable emission from the deep sea. PLoS One 3:e3766.

Walls GL (1931): The occurrence of colored lenses in the eyes of snakes and squirrels, and their probable significance. Copeia 1931:125-127.

Walls GL, Judd H (1933): The intra-ocular colour-filters of vertebrates. Br J Ophthalmol 17:641.

Watanabe H, Moku M, Kawaguchi K, Ishimaru K, Ohno A (1999): Diel vertical migration of myctophid fishes (Family Myctophidae) in the transitional waters of the western North Pacific. Fish Oceanogr 8:115-127.

Widder EA, Latz MI, Herring PJ, Case JF (1984): Far red bioluminescence from two deep-sea fishes. Science 225:512-514.

Widder EA (2002): Bioluminescence and the pelagic visual environment. Mar Freshw Behav Physiol 35:1-26.

Widder EA (2010): Bioluminescence in the ocean: origins of biological, chemical, and ecological diversity. Science 328:704-708.

Yokoyama R, Knox BE, Yokoyama S (1995): Rhodopsin from the fish, *Astyanax*: role of tyrosine 261 in the red shift. Invest Ophthalmol Vis Sci 36:939-945.

Yokoyama S, Tada T, Zhang H, Britt L (2008): Elucidation of phenotypic adaptations: Molecular analyses of dim-light vision proteins in vertebrates. Proc Natl Acad Sci 105:13480-13485.

Zeil J (1983): Sexual dimorphism in the visual system of flies: The compound eyes and neural superposition in bibionidae (Diptera). J Comp Physiol A 150:379-393.

Figure legends

Figure 1. Diversity in yellow pigmentation distribution across the retina of six species of lanternfishes. (*a-f*) Retinal wholemount visual observations. (*g-l*) Map of corrected absorbance at the wavelength of peak absorbance of the yellow pigmentation, λ_{YPmax}. (*a*, *g*) *Gonichthys tenuiculus*, (*b*, *h*) *Hygophum proximum*, (*c*, *i*) *Symbolophorus rufinus*, (*d*, *j*) *S. evermanni*, (*e*, *k*) *Myctophum lychnobium*, (*f*, *l*) *M. obtusirostre*. The white arrows indicate the orientation of the retina wholemount (T = temporal, V = ventral). Scale bars: 1 mm.

944

945 **Figure 2.** Location and distribution of the yellow pigmentation in the retina of
946 *Gonichthys tenuiculus*. PRL = Photoreceptor layer, ONL = outer nuclear layer, INL =
947 inner nuclear layer, GCL = ganglion cell layer. Scale bar: 50 μm.

948

949 **Figure 3.** Retinal wholemounts showing the sexual dimorphism in the yellow pigment in
950 two species of lanternfish. (*a*) *Myctophum brachyhnathum* and (*b*) *M. nitidulum*. The
951 yellow patch in the female *M. brachygnathum* is highlighted by a dotted line. The white
952 arrows indicate the orientation of the retina wholemount (T = temporal, V = ventral).
953 Scale bars: 1 mm.

954

955 **Figure 4.** Normalised corrected absorbance spectra of the yellow pigment in six
956 lanternfish species. (*a*) *Gonichthys tenuiculus*, λ_{YPmax} = 443 nm, (*b*) *Hygophum proximun*,
957 λ_{YPmax} = 381 nm, (*c*) *Symbolophorus rufinus*, λ_{YPmax} = 438 nm, (*d*) *S. evermanni*, λ_{YPmax} =
958 439 nm, (*e*) *Myctophum lychnobium*, λ_{YPmax} = 383 nm, (*f*) *M. obtusirostre*, λ_{YPmax} = 356
959 nm.

960

961 **Figure 5.** Mean bleaching difference absorbance spectra of the rod visual pigments in
962 three species of lanternfishes (*a*) *Symbolophorus evermanni*, (*b*) *Myctophum obtusirostre*,
963 (*c*) *M. spinosum*. The wavelength of maximum absorbance (λ_{max}) is also provided for
964 each species. Spectra (black lines) are fitted with visual pigment templates (grey lines,
965 [Govardovskii et al. 2000]) of appropriate λ_{max} value. For *M. obtusirostre* (*b*), the

966 absorbance spectra were measured in non-yellow and yellow pigmented areas of retinal
967 tissue.
968
969 **Figure 6.** Origin of the *Rh1* rod opsin gene duplication in *Symbolophorus evermanni*
970 within the Myctophidae. Phylogenetic trees were constructed by the (*a*) Neighbour-
971 Joining (Saitou and Nei 1987) and (*b*) Maximum Likelihood methods using *Rh1* opsin
972 gene nucleotide sequences of *Diaphus metopoclampu*s (JN544536), *Diaphus rafinesquii*
973 (JN412587), *Diaphus watasei* (JN231003), *Stenobrachius leucopsarus* (EU407251),
974 *Lampanyctus alatus* (JN412575), *Ceratoscopelus warmingii* (JN412573), *Bolinichthys*
975 *indicus* (JN412574), *Benthosema suborbitale* (JN412576), *Benthosema pterotum*
976 (JN231002), *Electrona antarctica* (AY141258), *Scopelarchus analis* (EF517404), *Danio*
977 *rerio* (HM367063), *Gymnocypris eckloni* (EU606010), and *Callorhinchus milii*
978 (EF565167). The *Rh2* opsin gene nucleotide sequence of *Danio rerio* (NM131253) was
979 added as a supplementary outgroup. The bootstrap confidence values are shown for each
980 branch. The scale bar is calibrated at 0.05 substitutions per site.
981
982 **Figure 7.** Modelling of the quantal spectral sensitivity of the two visual pigments
983 measured in *Myctophum obtusirostre*. (*a*) without the presence of the yellow
984 pigmentation and (*b*) with the yellow pigment associated with the long wave shifted
985 visual pigment (527 nm). Black line: 473 nm, grey line: 527 nm.
986
987 **Figure 8.** Modelling of the effect the yellow pigmentation on the quantal spectral
988 sensitivity of rod photoreceptors in *Symbolophorus evermanni*. (*a*) Quantal spectral

sensitivity of the three visual pigments (476 nm: black, 503 nm: dark grey, 512 nm: light grey) without the presence of the yellow pigmentation. (*b*-*d*) Different scenarios where the yellow pigment is associated with the two long wave-shifted visual pigments (*b*), the 503 nm visual pigment only (*c*) and the 512 nm visual pigment only (*d*).

Tables

Table 1. Summary of the individuals analysed in this study that presented a yellow patch of retinal tissue. For each individual, the sex (F = female, M = male, J = juvenile, ? = unknown), standard length (SL, in mm), eye diameter (eye ø, in mm), location of sampling and number of retinal yellow pigmented patch and their location (C = central, D = dorsal, T = temporal, N = nasal, V = ventral) is given.

Species	Sex	SL	Eye ø	Sampling location	Number of patch	Patch location
Myctophum brachygnathum	F	65.7	6.8	Coral Sea	1	C
	F	67.7	7.2	Coral Sea	1	C
	F	69.7	7.5	Coral Sea	1	C
	M	66.6	7.3	Coral Sea	1	T/V
	M	67.7	7.5	Coral Sea	1	T/V
	M	58.1	7.3	Hawaii	1	T/V
M. nitidulum	F	85.4	7.1	Peru-Chile Trench	1	T/C
	F	80.0	6.9	Peru-Chile Trench	1	T/C
	M	77.9	6.9	Peru-Chile Trench	1	N
M. obtusirostre	M	92.4	10.6	Coral Sea	1	V
	M	90.9	10.6	Coral Sea	1	V
M. lychnobium	F	106.1	11.1	Coral Sea	2	D + C/V
	F	83.3	9.4	Coral Sea	2	D + C/V
M. spinosum	F	87.5	8.7	Coral Sea	2	D + C/V
M. aurolaternatum	J	57.8	5.3	Coral Sea	1	V
Symbolophorus rufinus	J	73.7	6.6	Coral Sea	1	D
	J	62.5	6.1	Coral Sea	1	D
	J	31.6	2.8	Coral Sea	1	D
S. evermanni	J	65.8	6.7	Coral Sea	1	D
	J	53.8	4.8	Coral Sea	1	D
	J	48.1	4.5	Coral Sea	1	D
Gonichthys tenuiculus	M	49.4	3.5	Peru-Chile Trench	2	D + V
	?	43.1	2.9	Peru-Chile Trench	2	D + V
	?	40.6	2.7	Peru-Chile Trench	2	D + V
Hygophum proximum	J	43.3	5.2	Coral Sea	1	D

Table 2. Spectral absorption characteristics of rod visual pigments in the retina of three myctophids species measured using microspectrophotometry (MSP). [1] Maximum corrected absorbance measured at the λ_{max} of the bleaching difference spectrum. [2] Variable-point unweighted running average maximum of the data, which is a measure of the wavelength of peak absorbance of the pigment that is independent of any assumptions as to the type of chromophore (A1 or A2) present. Numbers in brackets represent the standard deviation (SD). λ_{max} values in nm.

	M. spinosum	***M. obtusirostre***		***S. evermanni***		
	1	1	2	1	2	3
Number of scans analysed	7	4	9	4	10	6
Chromophore	A1	A1	A2	A1	A1	A1+A2
Mean λ_{max} (± 1 std. dev.)	492.1 (±4.3)	473.4 (±1.7)	527.3 (±1.1)	475.9 (±1.2)	503.4 (±1.4)	512.7 (±7.4)
λ_{max} of the mean spectrum	492.4	473.2	526.5	476.0	503.5	511.9
Maximum corrected absorbance[1]	0.020	0.058	0.055	0.023	0.126	0.062
Running average[2] λ_{max}	494	477	528	477	505	510

Supplementary Material Legend

Detailed Materials and Methods for the spectrophotometry analyses.

Table S1. List of primer sets used in this study along with their annealing temperature (Ann. temp.) and the expected size of PR product. bp = base pair.

Figure S1. Normalised corrected absorbance spectra of the yellow pigment along with its maximum absorbance λ_{YPmax} and the full-width at half-maximum bandwidth (FWHM) in the lanternfish *Symbolophorus rufinus*. Measurements made from a paraformaldehyde-

fixed retina (black line) and an unfixed frozen retina (grey line) show that chemical fixation had only a small effect on the shape of the absorbance spectrum.

Figure S2. Phylogenetic trees of the two rod opsins found in the lanternfish *Symbolophorus evermanni*. The trees were constructed by (*a*) Neighbour-Joining (Saitou and Nei 1987) and (*b*) Maximum Likelihood methods using opsin gene nucleotide sequences of the zebrafish, *Danio rerio*: *Rh1-A* (HM367063), *Rh1-B* (HM367062), *Rh2-1* (NM131253), *Rh2-2* (NM182891), *Rh2-3* (NM182892), *Rh2-4* (NM131254), *SWS1* (NM131319), *SWS2* (NM131192), *LWS1* (NM131175), *LWS2* (NM001002443). The bootstrap confidence values are shown for each branch. The scale bar if calibrated at 0.1 substitutions per site.

Figure S3. Amino acids sequences of the two rod opsins identified in *Symbolophorus evermanni*. The two sequences (*Rh1A* and *Rh1B*) were aligned with *Stenobrachium leucopsarus* rod opsin sequence (EU407251). Identical residues are indicated by a dot, missing data by a dash. The black arrws indicate the tuning sites identified in *S. evermanni*.

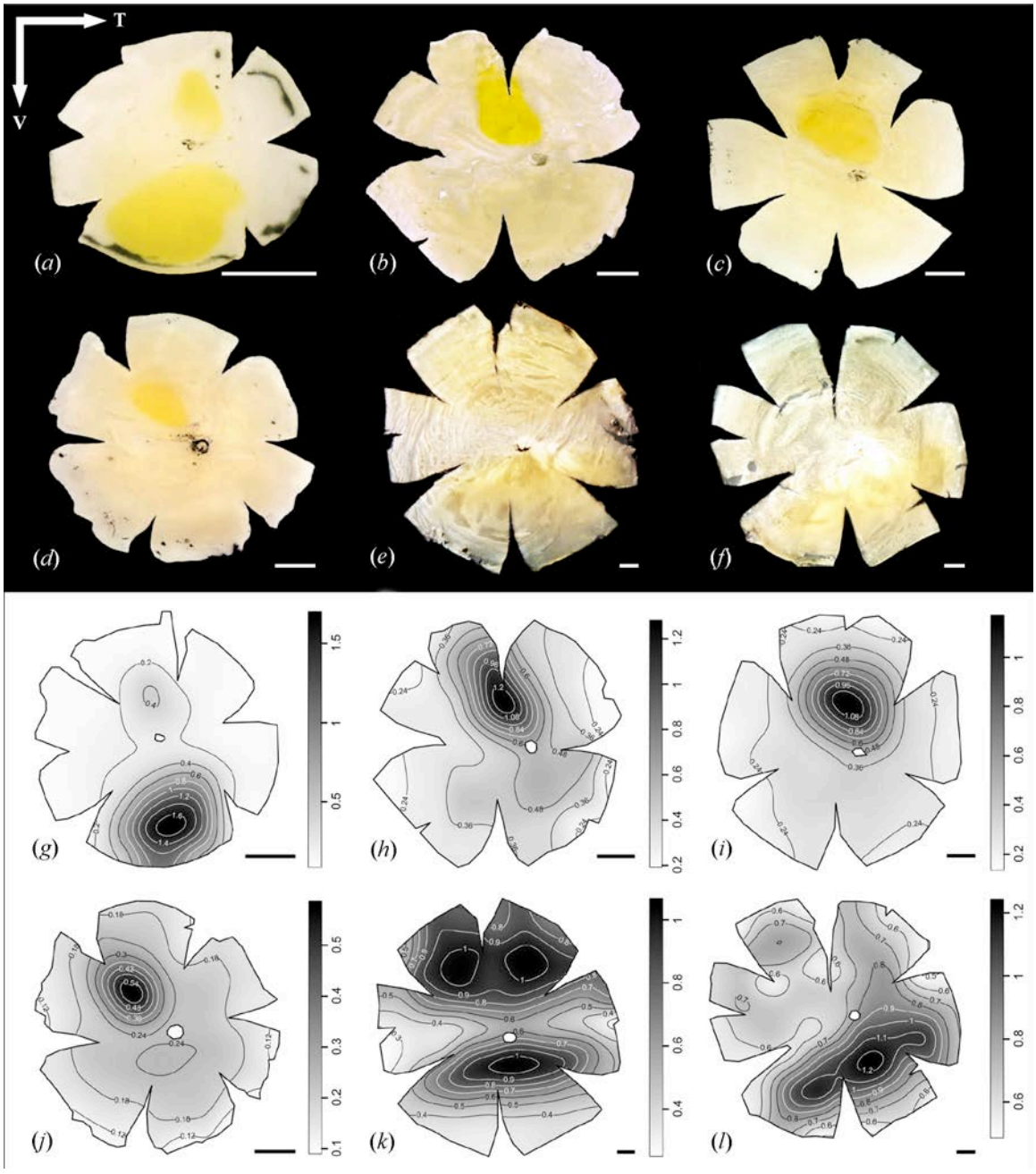

Figure 1. Diversity in yellow pigmentation distribution across the retina of six species of lanternfishes. (*a-f*) Retinal wholemount visual observations. (*g-l*) Map of corrected absorbance at the wavelength of peak absorbance of the yellow pigmentation, λ_{YPmax}. (*a*, *g*) *Gonichthys tenuiculus*, (*b*, *h*) *Hygophum proximum*, (*c*, *i*) *Symbolophorus rufinus*, (*d*, *j*) *S. evermanni*, (*e*, *k*) *Myctophum lychnobium*, (*f*, *l*) *M. obtusirostre*. The white arrows indicate the orientation of the retina wholemount (T = temporal, V = ventral). Scale bars: 1 mm.

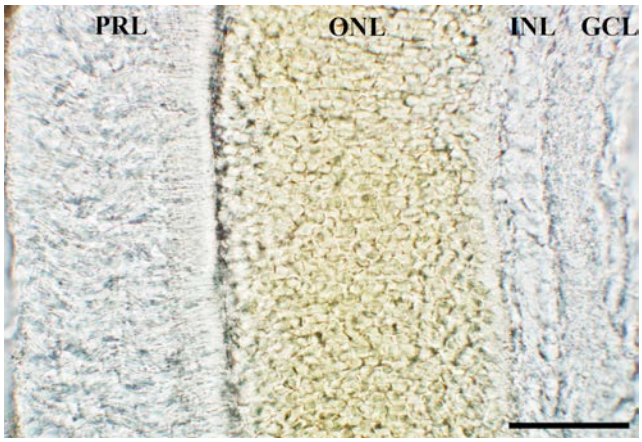

Figure 2. Location and distribution of the yellow pigmentation in the retina of *Gonichthys tenuiculus*. PRL = Photoreceptor layer, ONL = outer nuclear layer, INL = inner nuclear layer, GCL = ganglion cell layer. Scale bar: 50 μm.

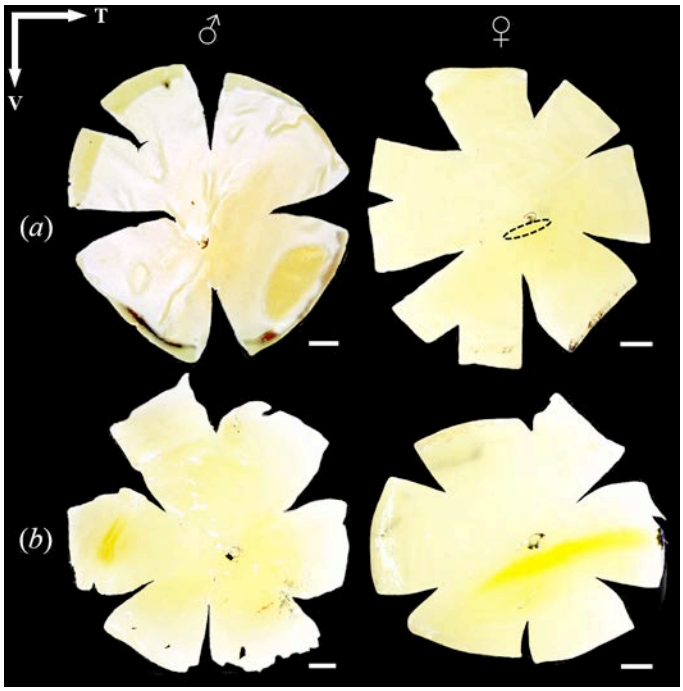

Figure 3. Retinal wholemounts showing the sexual dimorphism in the yellow pigment in two species of lanternfish. (*a*) *Myctophum brachyhnathum* and (*b*) *M. nitidulum*. The yellow patch in the female *M. brachygnathum* is highlighted by a dotted line. The white arrows indicate the orientation of the retina wholemount (T = temporal, V = ventral). Scale bars: 1 mm.

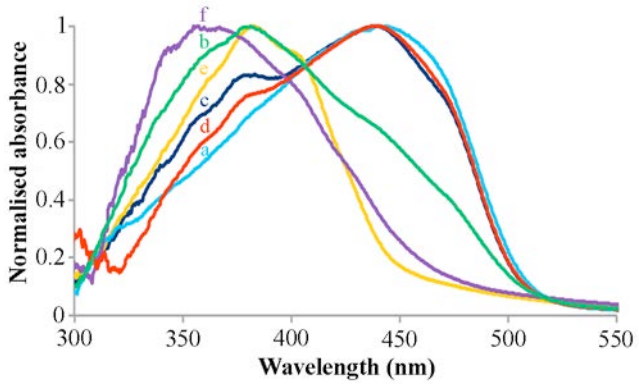

Figure 4. Normalised corrected absorbance spectra of the yellow pigment in six lanternfish species. (*a*) *Gonichthys tenuiculus*, λ_{YPmax} = 443 nm, (*b*) *Hygophum proximun*, λ_{YPmax} = 381 nm, (*c*) *Symbolophorus rufinus*, λ_{YPmax} = 438 nm, (*d*) *S. evermanni*, λ_{YPmax} = 439 nm, (*e*) *Myctophum lychnobium*, λ_{YPmax} = 383 nm, (*f*) *M. obtusirostre*, λ_{YPmax} = 356 nm.

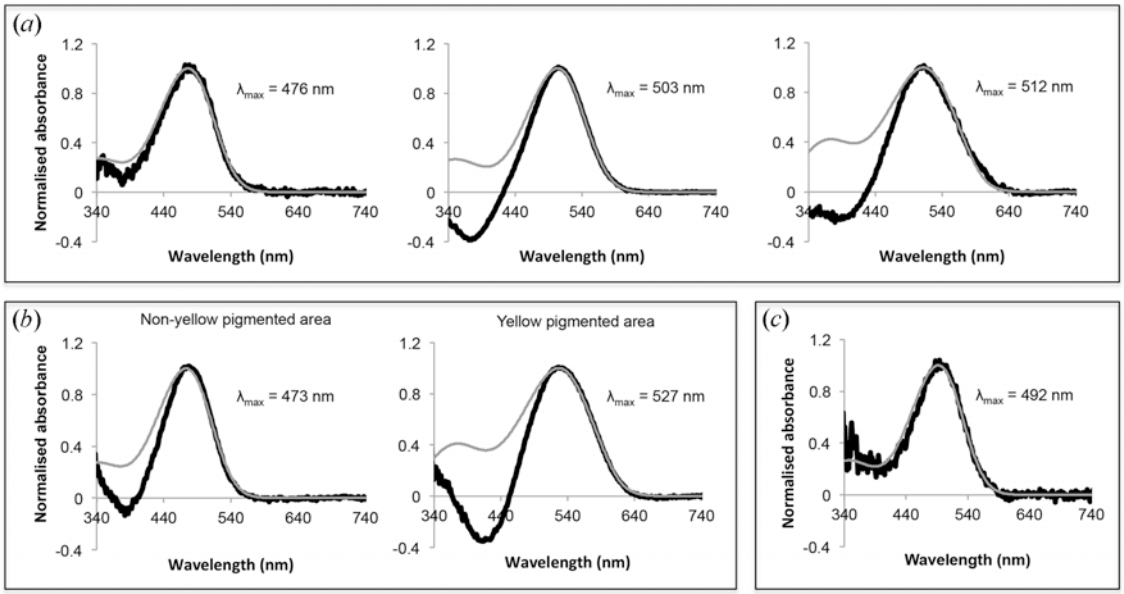

Figure 5. Mean bleaching difference absorbance spectra of the rod visual pigments in three species of lanternfishes (*a*) *Symbolophorus evermanni*, (*b*) *Myctophum obtusirostre*, (*c*) *M. spinosum*. The wavelength of maximum absorbance (λ_{max}) is also provided for each species. Spectra (black lines) are fitted with visual pigment templates (grey lines, [Govardovskii et al. 2000]) of appropriate λ_{max} value. For *M. obtusirostre* (*b*), the absorbance spectra were measured in non-yellow and yellow pigmented areas of retinal tissue.

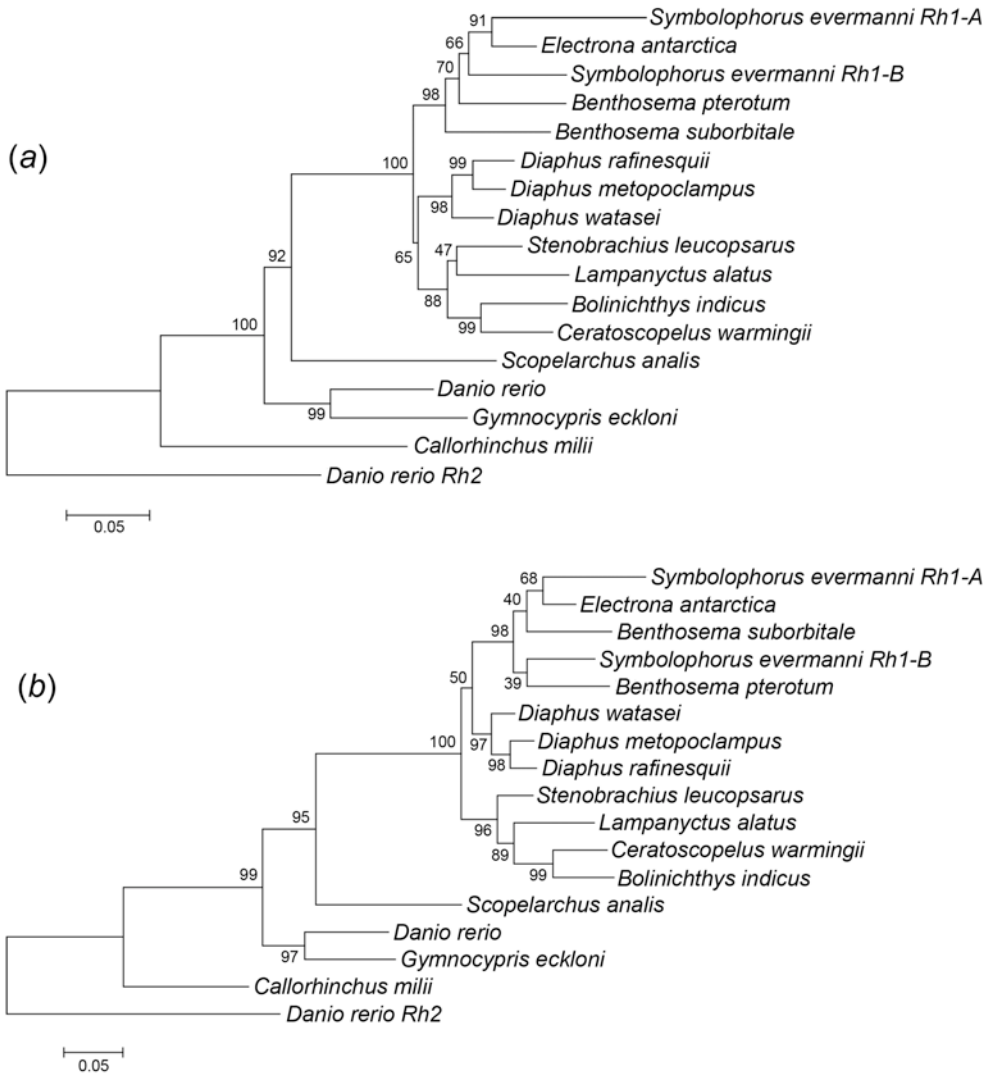

Figure 6. Origin of the *Rh1* rod opsin gene duplication in *Symbolophorus evermanni* within the Myctophidae. Phylogenetic trees were constructed by the (*a*) Neighbour-Joining (Saitou and Nei 1987) and (*b*) Maximum Likelihood methods using *Rh1* opsin gene nucleotide sequences of *Diaphus metopoclampu*s (JN544536), *Diaphus rafinesquii* (JN412587), *Diaphus watasei* (JN231003), *Stenobrachius leucopsarus* (EU407251), *Lampanyctus alatus* (JN412575), *Ceratoscopelus warmingii* (JN412573), *Bolinichthys indicus* (JN412574), *Benthosema suborbitale* (JN412576), *Benthosema pterotum* (JN231002), *Electrona antarctica* (AY141258), *Scopelarchus analis* (EF517404), *Danio rerio* (HM367063), *Gymnocypris eckloni* (EU606010), and *Callorhinchus milii* (EF565167). The *Rh2* opsin gene nucleotide sequence of *Danio rerio* (NM131253) was added as a supplementary outgroup. The bootstrap confidence values are shown for each branch. The scale bar is calibrated at 0.05 substitutions per site.

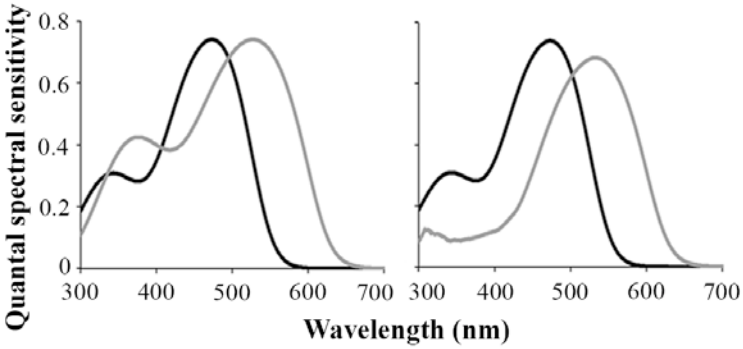

Figure 7. Modelling of the quantal spectral sensitivity of the two visual pigments measured in *Myctophum obtusirostre*. (*a*) without the presence of the yellow pigmentation and (*b*) with the yellow pigment associated with the long wave shifted visual pigment (527 nm). Black line: 473 nm, grey line: 527 nm.

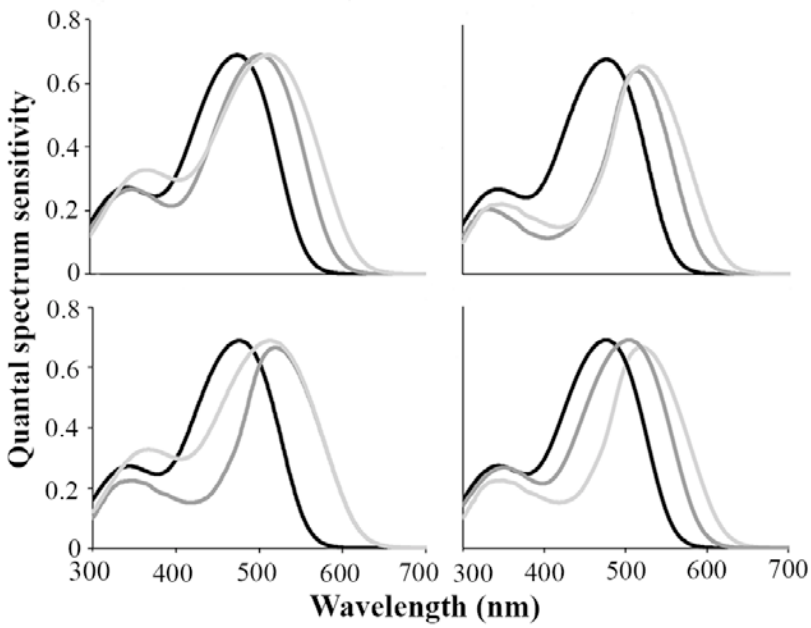

Figure 8. Modelling of the effect the yellow pigmentation on the quantal spectral sensitivity of rod photoreceptors in *Symbolophorus evermanni*. (*a*) Quantal spectral sensitivity of the three visual pigments (476 nm: black, 503 nm: dark grey, 512 nm: light grey) without the presence of the yellow pigmentation. (*b-d*) Different scenarios where the yellow pigment is associated with the two long wave-shifted visual pigments (*b*), the 503 nm visual pigment only (*c*) and the 512 nm visual pigment only (*d*).